Photonic Network Communications (2018) 36:279–288
https://doi.org/10.1007/s11107-018-0798-0

ORIGINAL PAPER

A cross-layer analysis of TCP/link adaptation technologies over free-space optical links with Markov error model

Chuyen T. Nguyen[1] · Hoang D. Le[2] · Vuong V. Mai[3]

Received: 5 September 2017 / Accepted: 29 August 2018 / Published online: 12 September 2018
© Springer Science+Business Media, LLC, part of Springer Nature 2018

Abstract
This paper presents a comprehensive cross-layer framework on the performance of transmission control protocol (TCP) over a free-space optical (FSO) link, which employs automatic repeat request (ARQ) and adaptive modulation and coding (AMC) schemes. Not similar to conventional works in the literature of FSO, we conduct a Markov error model to accurately capture effects of burst errors caused by atmospheric turbulence on cross-layer operations. From the framework, we quantify the impacts of different parameters/settings of ARQ, AMC, and the FSO link on TCP throughput performance. We also discuss several optimization aspects for TCP performance.

Keywords Free-space optical (FSO) communications · Atmospheric turbulence · TCP Reno · Markov error model

1 Introduction

Free-space optical (FSO) communication is an optical wireless communication technology based on the propagation of light in free space. Achieving data rates comparable to that of fiber optics without incurring exorbitant costs and requiring significant amount of time for installation, FSO is able to provide low-cost, time-constrained and high-bandwidth connectivity in various network scenarios [1].

In FSO links, one of the major performance-degrading factors, particularly for extended links, is the atmospheric turbulence [2]. The turbulence caused by solar heating and wind (even in a clear day) results in rapid fluctuations in both intensity and phase of the received signal and consequently degrades the reliability of FSO systems [3]. In order to cope with the issue, numerous techniques have been proposed in over the past decade. Among them, link adaptation technologies, such as automatic repeat request (ARQ) and adaptive modulation and coding (AMC) schemes, have recently received significant research attention due to advantages of efficiency and no additional physical infrastructures required. It is believed that link adaptation technologies will be indispensable components in the future FSO network architectures [4,5].

On the other hand, transmission control protocol (TCP) is a reliable transport protocol for many Internet applications, including FTP, Telnet, E-mail. Nevertheless, it has been proven that the TCP performance is severely degraded in high-error-rate environments, including both radio and optical wireless (e.g., FSO) communications. Therefore, such environments pose formidable challenges to maintain the TCP reliability [6–9].

1.1 Related works

In radio wireless communications, many proposals have been reported to overcome the degradation of TCP performance. It is seen in these studies that the existence of link adaptation technologies plays an important role in improving the TCP performance [6,7].

In FSO communications, several studies have also been devoted to modeling and evaluation of the TCP performance over FSO links. Nevertheless, in these works, the impacts of link adaptation technologies on improving the TCP performance were still not investigated thoroughly. In particular, Lee et al. focused solely on the transport layer and mathematically analyzed the TCP throughput over FSO without

✉ Chuyen T. Nguyen
chuyen.nguyenthanh@hust.edu.vn

1 School of Electronics and Telecommunications, Hanoi University of Science and Technology, Hanoi, Vietnam

2 School of Computer Science and Engineering, The University of Aizu, Aizuwakamatsu, Japan

3 School of Electrical Engineering, Korea Advanced Institute of Science and Technology (KAIST), Daejeon, South Korea

considering link adaptation technologies [9]. In other studies, there was the existence of ARQ, yet the transmission rate was assumed to be fixed; the authors then investigated TCP performance by using simulation tools and mathematical models (see in [10,11], respectively). The TCP performance over FSO links has also been experimentally studied by NEC Corporation [12], and again, link adaptation technologies were not considered in this work.

Furthermore, it is important to note that most existing analytical studies of TCP performance were often done with uniform error models [9–11] where the error structure of different block transmissions was assumed to be independent. Nevertheless, in FSO channels, because the temporal correlation time of the atmospheric turbulence process is of the order of several milliseconds, burst errors often occur during the transmission [13], i.e., the error structure is correlated. In the literature of wireless communications, it has also been proven that uniform models might not be suitable for representing the burst error patterns due to fading phenomena [14]. Instead, Markov chain models have been introduced in this situation to accurately describe the burst errors [15,16]. They, however, have not been considered so far in studies of TCP performance over FSO channels, which motivates us to propose this contribution.

1.2 Our contributions

This paper aims to provide *a comprehensive cross-layer performance analysis* for TCP over FSO links, in which both ARQ and AMC schemes are considered. It is worth mentioning that the understanding of combined effects of link adaptation technologies and FSO links on the TCP performance would be critical to design and optimize protocol parameter configurations for FSO networks under the harsh condition of atmospheric channels. The main contributions of this paper are threefold:

- First, we develop a link level model assuming ARQ at the link layer and AMC at the physical layer. This model, therefore, captures important aspects of future FSO links architecture. It removes the limitations of existing works, which assumed either no link adaptation technologies or only ARQ employed.
- Second, we provide a more accurate performance analysis of TCP over FSO channels. Instead of using the uniform error model, we take into account the nature of burst error through using a Markov chain error model.
- Through our evaluation framework, we evaluate and optimize TCP performance. Specifically, we quantify the impacts of different parameters/settings of ARQ, AMC and FSO links on TCP throughput performance. We then discuss several optimization aspects for TCP performance.

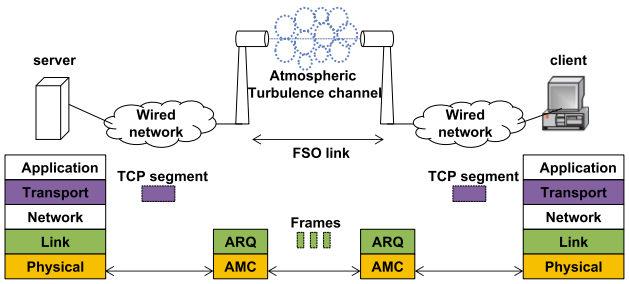

Fig. 1 Network scenario with a TCP connection over FSO link employing ARQ and AMC

In practical scenarios where FSO link is a part of the whole network connection, it is expected that our framework could help Internet service providers and network designers in qualifying TCP performance. Actually, suggestions to improving the TCP performance can also be provided through our work.

2 Network model

2.1 Network description

Figure 1 illustrates our considered end-to-end network scenario between a TCP server and a client over wired networks and an FSO link. The data are transmitted from the server to the client, which will be presented in details through network layers. The application and network layers are, nevertheless, supposed to be ignored since this work focuses on the TCP performance with effects of FSO atmospheric turbulence.

At the *transport layer*, one of the TCP variants is implemented, and in this paper, we adopt TCP Reno without loss of generality [17]. The performance of the others can be analyzed in the same way. The operation of TCP Reno is mainly based on the additive increase and multiplicative decrease (AIMD) algorithm, which combines linear growth of the congestion window with an exponential reduction when congestion takes place [18]. The transmitted data unit in this layer is segment with a size of L_{TCP}. Each segment will be then divided into N_f small data units, i.e., frames for the data transmission at lower layers.

At the *data link layer*, ARQ protocol is implemented. During the data transmission, frame errors might happen, and the server does not receive any acknowledgment (ACK) before a predefined timeout. In this case, it keeps re-transmitting the frame until the ACK is successfully received. If the frame does not get through the networks after M re-transmissions, the corresponding TCP segment is assumed to be lost.

At the *physical layer*, data are transmitted frame by frame over wired and FSO links. In this paper, we focus on the FSO channel to analyze the effects of the atmospheric turbulence

on the TCP performance. In particular, it is widely known in the literature that the FSO channel can be modeled as a random process with gamma–gamma distribution in which the probability density function (pdf) of the signal-to-noise ratio (SNR) is expressed as [19]

$$f_\gamma(\gamma) = \frac{(\alpha\beta)^{\frac{\alpha+\beta}{2}}}{\Gamma(\alpha)\Gamma(\beta)\bar{\gamma}^{\frac{\alpha+\beta}{4}}}\gamma^{\frac{\alpha+\beta}{4}-1}K_{\alpha-\beta}\left(2\sqrt{\alpha\beta\sqrt{\frac{\gamma}{\bar{\gamma}}}}\right), \tag{1}$$

where γ and $\bar{\gamma}$ are the instantaneous and average SNRs, respectively. $\Gamma(.)$ is the gamma function and $K_{\alpha-\beta}(.)$ is the modified Bessel function of the second kind and order $\alpha-\beta$. Parameters α and β describe the turbulence experienced by waves, and in the case of zero-inner scale, they are given by

$$\alpha = \left\{\exp\left[\frac{0.49\sigma_R^2}{\left(1+1.11\sigma_R^{12/5}\right)^{7/6}}\right]-1\right\}^{-1},$$
$$\beta = \left\{\exp\left[\frac{0.51\sigma_R^2}{\left(1+0.69\sigma_R^{12/5}\right)^{5/6}}\right]-1\right\}^{-1}. \tag{2}$$

Here, σ_R^2 is the Rytov variance, and in the case of plane wave propagation, it is given by

$$\sigma_R^2 = 1.23C_n^2k^{7/6}L^{11/6}, \tag{3}$$

where C_n^2 is the altitude-dependent index of refractive structure parameter, and it typically varies from 10^{-17} to 10^{-13} accordingly to the atmospheric turbulence strength. L is the channel distance, and $k = 2\pi/\lambda$ is the optical wave number [20]. The cumulative distribution function (cdf) denoted by $F_\gamma(\gamma)$ of γ can be also written as

$$F_\gamma(\gamma) = \frac{1}{\Gamma(\alpha)\Gamma(\beta)} \times G_{1,3}^{2,1}\left[\alpha\beta\sqrt{\frac{\gamma}{\bar{\gamma}}}\,|_{\alpha,\beta,0}^{1}\right], \tag{4}$$

where $G_{1,3}^{2,1}[\cdot]$ is the Meijer's G-function [21].

2.2 Adaptive modulation and coding (AMC)

In order to cope with the atmospheric turbulence, the adaptive modulation and coding (AMC) technique is employed at the physical layer. The purpose of AMC is to maximize the data rate by controlling transmission parameters based on channel conditions, while maintaining a predefined frame error rate P_{target}. In this paper, P_{target} is supposed to used for a given quality of service (QoS), and is determined as

$$P_{\text{target}} := P_{\text{loss}}^{\frac{1}{M+1}}, \tag{5}$$

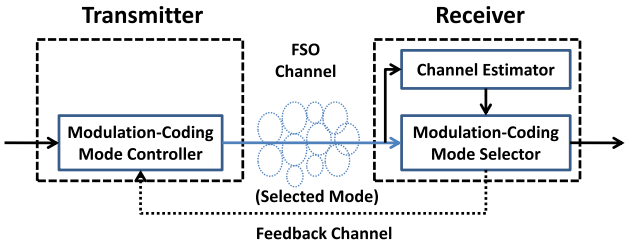

Fig. 2 AMC scheme to cope with atmospheric turbulence

where P_{loss} is the required maximum frame error rate at the physical layer after M re-transmissions [22]. We describe the operation of AMC schemes in detail in Fig. 2. There is an AMC controller at the transmitter, while an AMC selector is employed at the receiver. Different transmission modes with different transmission rates are available, where each mode is represented by a standard modulation and coding format. Based on estimated channel state information (CSI), assumed to be perfect in this paper, the AMC controller can select suitable transmission modes. Table 1 shows an example of AMC with $N = 5$ transmission modes which employs convolutionally coded M_n-ary QAM, adopted from the HIPERLAN/2 or the IEEE 802.11a standards [23]. We also use this example for further performance evaluation, while other examples can be similarly constructed.

We separate the entire SNR range into $N+1$ intervals with boundary points denoted as $\{\gamma_n\}_{n=0}^{N+1}$, where n is the mode index. Transmission mode n is selected if $\gamma \in [\gamma_n, \gamma_{n+1})$. No transmission is allowed when $\gamma < \gamma_1$ to avoid high frame error rate (FER). The algorithm searching for the thresholds $\{\gamma_n\}_{n=0}^{N+1}$ to achieve P_{target} is as

$$\gamma_0 = 0,$$
$$\gamma_n = \frac{1}{g_n}\ln\left(\frac{a_n}{P_{\text{target}}}\right),$$
$$\gamma_{N+1} = +\infty, \tag{6}$$

where a_n and g_n are the mode-dependent parameters, which we can see in Table 1 [24].

3 Finite-state Markov channel model

In this section, we adopt a finite-state Markov model to capture characteristics of the considered FSO channel. In particular, the FSO channel along with five different transmission modes in Table 1 can be modeled as a Markov chain of six states as shown in Fig. 3 [25]. The channel is in state n ($n = 0,\ 1,\ 2,\ 3,\ 4,\ 5$) if the received SNR falls into the interval of $[\gamma_n, \gamma_{n+1})$ where $\gamma_0 = 0$ and $\gamma_6 = +\infty$. In other words, the probability that the channel is in state n denoted by $\Pr_n$ can be written as

Table 1 Transmission modes with convolutionally coded modulation

	TM 1	TM 2	TM 3	TM 4	TM 5
Modulations	BPSK	QPSK	8-QAM	16-QAM	32-QAM
Coding rate R_c	1/2	1/2	3/4	3/4	3/4
R_n (bits/symbol)	1	2	3	4	5
a_n	67.7328	73.8279	58.7332	55.9137	50.0552
g_n	0.9819	0.4945	0.1641	0.0989	0.0381
γ_{pn} (dB)	6.3281	9.3945	13.9470	16.0938	20.1103

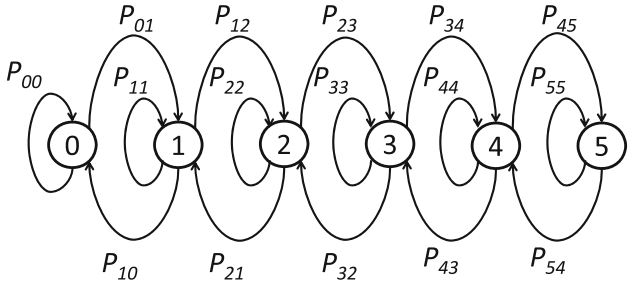

Fig. 3 Finite-state Markov channel model

$$\mathrm{Pr}_n = \int_{\gamma_n}^{\gamma_{n+1}} f_\gamma(\gamma)\mathrm{d}\gamma = F_\gamma(\gamma_{n+1}) - F_\gamma(\gamma_n), \tag{7}$$

where $f_\gamma(\gamma)$ and $F_\gamma(\gamma)$ are found in (1) and (4), respectively.

Under the characteristics of slow-fading channel, we assume that the transitions only happen between adjacent modes. As a result, the probabilities of moving from mode n to mode l can be computed as follows [26]

$$\begin{aligned} p_{n,n+1} &= \frac{N(\gamma_{n+1})T_f}{\mathrm{Pr}_n}, && \text{if } n = 0,\ldots,N-1,\\ p_{n,n-1} &= \frac{N(\gamma_n)T_f}{\mathrm{Pr}_n}, && \text{if } n = 1,\ldots,N,\\ p_{n,l} &= 0, && \text{if } |l-n| \geq 2, \end{aligned} \tag{8}$$

where $T_f = \frac{L_f}{R_s R_n}$ is the frame transmission time at mode n in which R_n (bits/symbol) is the information rate, L_f (bits) is the frame size, and R_s (symbols/s) is the fixed symbol rate. $N(\gamma_n)$ is the level crossing rate of signal level of γ_n during the SNR process, in the positive direction only (or in the negative direction only), which can be written as follows [5]

$$N(\gamma_n) = \frac{1}{4\pi t_0}\exp\left[\frac{1}{2\left(1-e^{4\sigma_s^2}\right)}\left(\frac{\gamma_n-\overline{\gamma}}{\overline{\gamma}}\right)^2\right], \tag{9}$$

where t_0 is the coherence time and σ_s^2 is log intensity variance. σ_s^2 describes the strength of the turbulence and can be expressed by [27]

$$\sigma_s^2 = \exp\left(\frac{0.49\sigma_R^2}{\left(1+0.18d^2+0.56\sigma_R^{12/5}\right)^{7/6}} + \frac{0.51\sigma_R^2}{\left(1+0.9d^2+0.62\sigma_R^{12/5}\right)^{5/6}}\right) - 1, \tag{10}$$

where $d = \sqrt{kD^2/4L}$. k, D and L are the optical wave number, receiver aperture diameter and channel distance, respectively. In addition, the probabilities of staying at the same state n can be written as follows:

$$p_{n,n} = \begin{cases} 1-p_{n,n+1}-p_{n,n-1}, & \text{if } 0 < n < N,\\ 1-p_{0,1}, & \text{if } n = 0,\\ 1-p_{N,N-1}, & \text{if } n = N. \end{cases} \tag{11}$$

In summary, the transition probabilities can be represented in a $(N+1)$ by $(N+1)$ matrix of $\mathbf{P}$ as

$$\mathbf{P} = \begin{bmatrix} p_{0,0} & p_{0,1} & \cdots & 0\\ p_{1,0} & p_{1,1} & p_{1,2} & \vdots\\ 0 & \ddots & \ddots & 0\\ \vdots & \cdots & p_{N-1,N-1} & p_{N-1,N}\\ 0 & \cdots & p_{N,N-1} & p_{N,N} \end{bmatrix}. \tag{12}$$

We now find the average frame error rate at each state n, which is denoted by $\overline{\mathrm{FER}}_n$. In particular, according to [17], it is approximately found as

$$\begin{aligned} \overline{\mathrm{FER}}_n &\simeq \frac{a_n}{\mathrm{Pr}_n}\int_{\gamma_n}^{\gamma_{n+1}} e^{-g_n\gamma} f_\gamma(\gamma)\mathrm{d}\gamma\\ &= \frac{a_n B(\alpha-\beta, 1-\alpha+\beta)}{2\mathrm{Pr}_n\Gamma(\alpha)\Gamma(\beta)}(X-Y), \end{aligned} \tag{13}$$

where $B(x,y) = \frac{\Gamma(x)\Gamma(y)}{\Gamma(x+y)}$ is the Beta function. In addition,

$$X = \sum_{p=0}^{\infty} \frac{a_p(\alpha,\beta)}{\bar{\gamma}^{\frac{p+\beta}{2}} g_n^{\frac{p+\beta}{2}}} \times \left[\Gamma\left(\frac{p+\beta}{2}, g_n\gamma_n\right) - \Gamma\left(\frac{p+\beta}{2}, g_n\gamma_{n+1}\right)\right], \tag{14}$$

and

$$Y = \sum_{p=0}^{\infty} \frac{a_p(\beta,\alpha)}{\bar{\gamma}^{\frac{p+\beta}{2}} g_n^{\frac{p+\alpha}{2}}} \times \left[\Gamma\left(\frac{p+\alpha}{2}, g_n\gamma_n\right) - \Gamma\left(\frac{p+\alpha}{2}, g_n\gamma_{n+1}\right)\right], \tag{15}$$

where $\Gamma(m,k)$ is the complementary incomplete Gamma function, i.e., $\Gamma(m,k) = \int_k^{\infty} t^{m-1}e^{-t}\mathrm{d}t$, while $a_p(x,y)$ is given by

$$a_p(x,y) = \frac{(xy)^{p+y}}{\Gamma(p-x+y+1)p!}. \tag{16}$$

4 Throughput performance analysis with Markov error model

In this section, we study the TCP performance with impacts of different parameters settings of ARQ, AMC and FSO links. In particular, instead of using uniform error model as in previous works, we adopt a Markov error model extended from the conventional Gilbert–Elliot scheme [28] to accurately analyze the average TCP throughput. The model is especially suitable to FSO systems with slow-fading channels.

4.1 Markov error model analysis

Our Markov error model is shown in Fig. 4 with N different *Good* states, which correspond to N transmission modes, and a *Bad* state denoted by $\mathrm{G}_k, k \in \{1,\ldots,N\}$ and B, respectively. In state G_k, frames are successfully transmitted, while in state B, they are all in error. Here, we use only one state as the common bad state for all transmission modes to reduce the complexity of the error model, thus simplifying the performance analysis. As a result, transitions might occur between the bad state and any good state. Nevertheless, the transition within good states is supposed to only occur between adjacent ones due to the assumption of a slow-fading channel. According to [28], the state transition probabilities between B and B, B and G_k, G_k and B, G_k and G_h denoted by q_{BB}, q_{BG_k}, $q_{\mathrm{G}_k\mathrm{B}}$, $q_{\mathrm{G}_k\mathrm{G}_h}$, respectively, can be calculated as

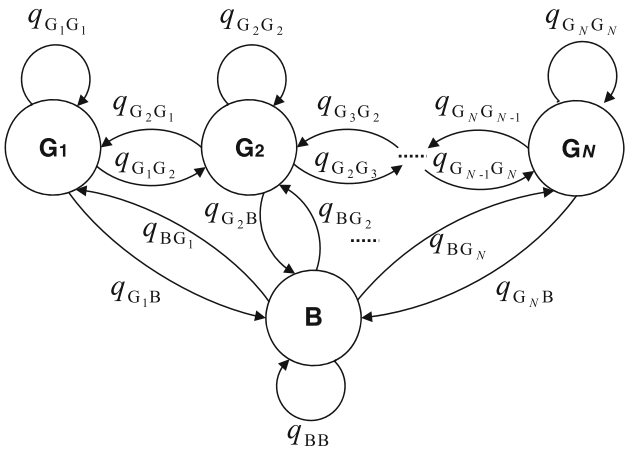

Fig. 4 Markov error model with N good states and one bad state

$$\begin{aligned} q_{\mathrm{BB}} &= \Pr\{\text{state B at } t=n+1 | \text{state B at } t=n\} \\ &= \frac{\Pr\{\text{state B at } t=n+1,\ \text{state B at } t=n\}}{\Pr\{\text{state B at } t=n\}} \\ &= \frac{\sum_{n=1}^{N}\sum_{l=1}^{N}\Pr_n\overline{\mathrm{FER}}_n\, p_{n,l}\overline{\mathrm{FER}}_l}{\sum_{n=1}^{N}\Pr_n\overline{\mathrm{FER}}_n}. \end{aligned} \tag{17}$$

$$\begin{aligned} q_{\mathrm{BG}_k} &= \Pr\{\text{state G}_k \text{ at } t=n+1 | \text{state B at } t=n\} \\ &= \frac{\Pr\{\text{state G}_k \text{ at } t=n+1,\ \text{state B at } t=n\}}{\Pr\{\text{state B at } t=n\}} \\ &= \frac{\sum_{n=1}^{N}\Pr_n\overline{\mathrm{FER}}_n\, p_{n,k}\left(1-\overline{\mathrm{FER}}_k\right)}{\sum_{n=1}^{N}\Pr_n\overline{\mathrm{FER}}_n}. \end{aligned} \tag{18}$$

$$\begin{aligned} q_{\mathrm{G}_k\mathrm{B}} &= \Pr\{\text{state B at } t=n+1 | \text{state G}_k \text{ at } t=n\} \\ &= \frac{\Pr\{\text{state B at } t=n+1,\ \text{state G}_k \text{ at } t=n\}}{\Pr\{\text{state G}_k \text{ at } t=n\}} \\ &= \frac{\sum_{n=1}^{N}\Pr_k\left(1-\overline{\mathrm{FER}}_k\right)p_{k,n}\overline{\mathrm{FER}}_n}{\Pr_k\left(1-\overline{\mathrm{FER}}_k\right)}. \end{aligned} \tag{19}$$

$$\begin{aligned} q_{\mathrm{G}_k,\mathrm{G}_h} &= \Pr\{\text{state G}_h \text{ at } t=n+1 | \text{state G}_k \text{ at } t=n\} \\ &= \frac{\Pr\{\text{state G}_h \text{ at } t=n+1,\ \text{state G}_k \text{ at t } =n\}}{\Pr\{\text{state G}_k \text{ at } t=n\}} \\ &= \frac{\Pr_k\left(1-\overline{\mathrm{FER}}_k\right)p_{k,h}\left(1-\overline{\mathrm{FER}}_h\right)}{\Pr_k\left(1-\overline{\mathrm{FER}}_k\right)}, \end{aligned} \tag{20}$$

where $k,h \in \{1,\ldots,N\}$. We can also re-write transition probabilities in a matrix form of $\mathbf{Q}$ as follows:

$$\mathbf{Q} = \begin{bmatrix} \mathbf{Q}_{\mathrm{BB}} & \mathbf{Q}_{\mathrm{BG}} \\ \mathbf{Q}_{\mathrm{GB}} & \mathbf{Q}_{\mathrm{GG}} \end{bmatrix}$$

$$= \begin{bmatrix} q_{\mathrm{BB}} & q_{\mathrm{BG}_1} & \cdots & q_{\mathrm{BG}_{N-1}} & q_{\mathrm{BG}_N} \\ q_{\mathrm{G}_1\mathrm{B}} & q_{\mathrm{G}_1\mathrm{G}_1} & \cdots & 0 & 0 \\ q_{\mathrm{G}_2\mathrm{B}} & q_{\mathrm{G}_2\mathrm{G}_1} & \cdots & 0 & 0 \\ q_{\mathrm{G}_3\mathrm{B}} & 0 & \cdots & 0 & 0 \\ \cdots & \cdots & \cdots & \cdots & \cdots \\ q_{\mathrm{G}_{N-1}\mathrm{B}} & 0 & \cdots & q_{\mathrm{G}_{N-1}\mathrm{G}_{N-1}} & q_{\mathrm{G}_{N-1}G_N} \\ q_{\mathrm{G}_N\mathrm{B}} & 0 & \cdots & q_{\mathrm{G}_N\mathrm{G}_{N-1}} & q_{\mathrm{G}_N\mathrm{G}_N} \end{bmatrix}. \quad (21)$$

We then denote by q_{B} and q_{G_k} the stationary probabilities of state B and state G_k, respectively, and $\mathbf{q} = [q_{\mathrm{B}}, q_{\mathrm{G}_1}, q_{\mathrm{G}_2}, ..., q_{\mathrm{G}_N}]$. According to the Markov chain theory, we have

$$\begin{cases} \mathbf{q} = \mathbf{q}.\mathbf{Q}, \\ q_{\mathrm{B}} + \sum_{k=1}^{N} q_{\mathrm{G}_k} = 1. \end{cases} \quad (22)$$

By solving (22), we can easily obtain $\mathbf{q}$.

4.2 Average frame error rate

Based on the error model analyzed in the previous subsection, we can find the average FER defined as the ratio between the average number of frames transmitted in state B (N_{B}) and the total one (N_t) transmitted in all states, i.e.,

$$\overline{\mathrm{FER}} = \frac{N_{\mathrm{B}}}{N_t}, \quad (23)$$

where $\overline{\mathrm{FER}}$ is the average FER. To do this, we now determine N_{B} and N_t. In particular, given a period of time, N_t can be computed as follows:

$$N_t = N_{\mathrm{B}} + \sum_{k=1}^{N} N_{\mathrm{G}_k}, \quad (24)$$

where N_{G_k} is the average number of frames transmitted in state G_k. It can be determined by

$$N_{\mathrm{G}_k} = q_{\mathrm{G}_k} R_{fk} \overline{\tau}_k, \quad (25)$$

where q_{G_k} can be found via (22), R_{fk} (frames/s) is the transmission rate in channel state k and can be defined as

$$R_{fk} = \frac{R_s \times R_k}{L_f}, \quad k = 1, 2, \ldots, N, \quad (26)$$

where R_s, R_k, and L_f are the symbol rate, information rate, and frame size, respectively. $\overline{\tau}_k$ is the average time duration in channel state k, $k = 1, 2, \ldots, N$, which is given as [28]

$$\overline{\tau}_k = \frac{\mathrm{Pr}_k}{N(\gamma_k) + N(\gamma_{k+1})}, \quad (27)$$

where Pr_k and $N(\gamma_k)$ are determined in (7) and (9), respectively.

Besides, since frames transmitted in state B are all erroneous, N_{B} can be calculated by

$$N_{\mathrm{B}} = q_{\mathrm{B}} R_{f\mathrm{B}} \overline{\tau}_{\mathrm{B}}, \quad (28)$$

where q_{B} is determined via (22). $R_{f\mathrm{B}}$ and $\overline{\tau}_{\mathrm{B}}$ are the average transmission rate and average time duration in state B, respectively. They can be computed as follows:

$$R_{f\mathrm{B}} = \sum_{k=1}^{N} \mathrm{Pr}_k R_{fk}, \quad (29)$$

and

$$\overline{\tau}_{\mathrm{B}} = \sum_{k=1}^{N} \mathrm{Pr}_k \overline{\tau}_k. \quad (30)$$

Finally, by substituting (24), (25) and (28) into (23), we can obtain the average FER.

4.3 TCP throughput performance analysis

According to [29], the TCP Reno throughput denoted by η can be approximately written as follows:

$$\eta = \min \left(\frac{W_{\max}}{\mathbf{E}[\mathrm{RTT}]}, \frac{1}{\mathbf{E}[\mathrm{RTT}]\sqrt{\frac{4\mathbb{P}}{3}} + T_0 \min\left(1, 3\sqrt{\frac{3\mathbb{P}}{4}}\right) \mathbb{P}\left(1 + 32\mathbb{P}^2\right)} \right), \quad (31)$$

where $W_{\max}$ is the maximum window size, $\mathbf{E}[\mathrm{RTT}]$ is the average round-trip time, T_0 is the initial time-out duration, and $\mathbb{P}$ is the TCP segment loss probability. To find η, we now calculate $\mathbf{E}[\mathrm{RTT}]$ and $\mathbb{P}$. In particular, $\mathbf{E}[\mathrm{RTT}]$ can be approximately obtained according to [29] as follows:

$$\mathbf{E}[\mathrm{RTT}] \approx 2T_{\mathrm{wire}} + (L_f/\overline{R}_b + T_{\mathrm{CRC}})(\overline{M} + 1), \quad (32)$$

where T_{wire} is one-way transmission time in the wired network and T_{CRC} is the error detection time. $L_f/\overline{R}_b$ is the time to transmit a frame, while L_f is the frame length, $\overline{R}_b$ (bps) is the average bit error rate which can be defined as

$$\overline{R}_b = \sum_{k=1}^{N} \mathrm{Pr}_k R_s R_n, \quad (33)$$

Table 2 System parameters

Name	Symbol	Value
TCP segment size	L_{TCP}	1500 bytes
Frame size	L_f	500 bytes
CRC checking time	T_{CRC}	20 μs
One-way trans. time in wired networks	T_{wire}	1 μs
The maximum bit rate	$R_{b\max}$	1 Gbps
Segment loss of the wired network	P_{wire}	0
Symbol rate	R_s	2×10^8 Symbols/s
Receiver aperture diameter	D	0.02 m
Optical wave length	λ	1.55 μm
Coherence time	t_0	1 ms

In addition, $\overline{M}$ is the average number of re-transmissions per frame and is calculated as

$$\overline{M} = \frac{\overline{\text{FER}}}{1-\overline{\text{FER}}} - \frac{(M+1)\overline{\text{FER}}^{M+1}}{1-\overline{\text{FER}}^{M+1}}. \tag{34}$$

On the other hand, let P_{FSO} and P_{wire} denote by the segment loss probabilities in the FSO link and the wired network, respectively. The TCP segment loss probability $\mathbb{P}$ can be then expressed as

$$\mathbb{P} = 1 - (1 - P_{\text{FSO}})(1 - P_{\text{wire}}), \tag{35}$$

where $P_{\text{FSO}} = 1 - \left(1 - \overline{\text{FER}}^{M+1}\right)^{N_f}$. Substituting (32) and (35) into (31), we can obtain the TCP throughput.

5 Numerical results and discussion

In this section, the TCP throughput performance is evaluated with different settings of ARQ, AMC schemes. System parameters related to TCP and the link layer are described in Table 2. Here, to focus on the effects of the FSO atmospheric turbulence on the TCP performance, we assume that (i) there is no segment loss in the wired networks and (ii) the one-way transmission time of wired network and CRC checking time are assumed in order of μs that causes a relatively low delay. The data unit sizes (TCP segment and frame) are set as recommended by the standard Ethernet (IEEE 802.3).

We first plot in Fig. 5 the Reno throughput performance with respect to different values of SNR for given $M = 1$, $P_{\text{loss}} = 10^{-6}$, and $L = 1500$ m. Regarding the FSO channel, we assume that $C_n^2 = 7 \times 10^{-15}\,\text{m}^{-2/3}$, $C_n^2 = 3 \times 10^{-14}\,\text{m}^{-2/3}$, and $C_n^2 = 6 \times 10^{-14}\ \text{m}^{-2/3}$ represent for the weak, moderate and strong turbulence, respectively. We can see that as the SNR increases, the throughput increases until it reaches a limit determined by the maximum window size

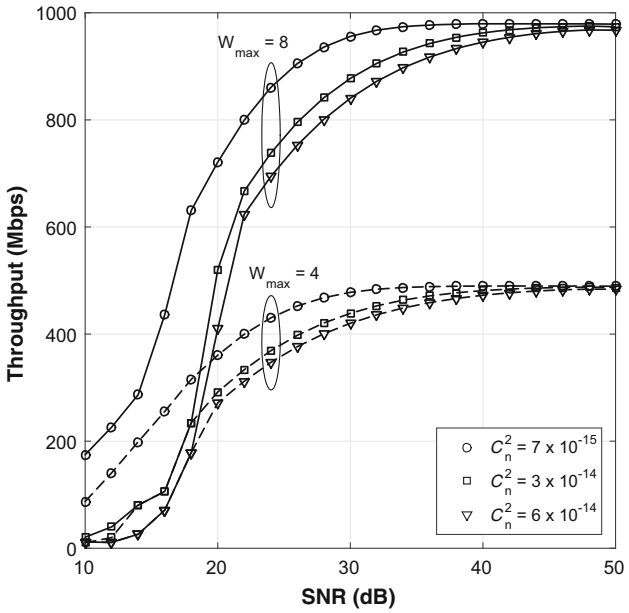

Fig. 5 TCP throughput versus average SNR under different conditions of atmospheric turbulence, given $M = 1$, $P_{\text{loss}} = 10^{-6}$, $L = 1500$m

$W_{\max}$ (4 or 8 segments in our case). In addition, it is understandable to see that an increase in turbulence strength results in an increase in required SNR to achieve the same throughput. For example, given $W_{\max} = 8$ the required SNRs to achieve the maximum throughput are 34, 42 and 44 dB for weak, moderate and strong turbulence, respectively.

We now study the impacts of ARQ protocol on the TCP performance via Fig. 6. Here, the throughput is evaluated over a moderate turbulence FSO channel with different values of M, given $C_n^2 = 3 \times 10^{-14}\,\text{m}^{-2/3}$, $P_{\text{loss}} = 10^{-6}$, $L = 1500$ m. It is to evidently observe the advantage of ARQ in improving the throughput performance. In particular, when ARQ with $M = 1$ is employed, the throughput can be achieved over 800 Mbps at SNR = 30 dB, whereas that without ARQ is only 400 Mbps for the same SNR. Nevertheless, the use of ARQ also significantly increases the average end-to-end

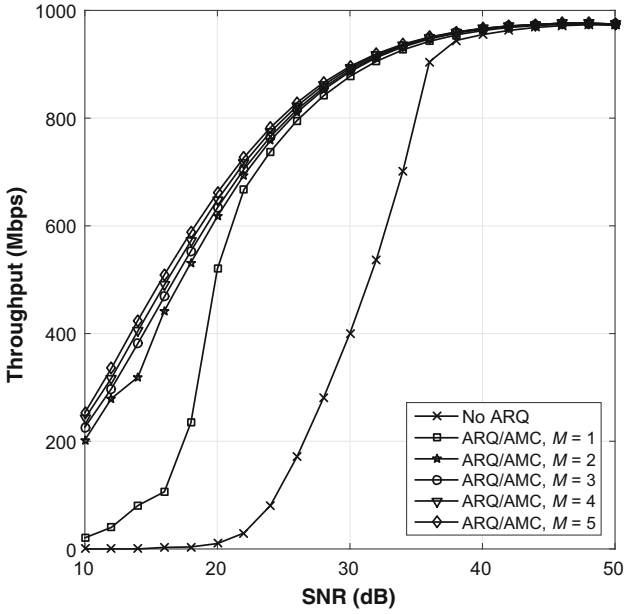

Fig. 6 TCP throughput versus average SNR with different values of M, given $C_n^2 = 3 \times 10^{-14}\,\mathrm{m}^{-2/3}$, $P_{\mathrm{loss}} = 10^{-6}$, $L = 1500\,\mathrm{m}$

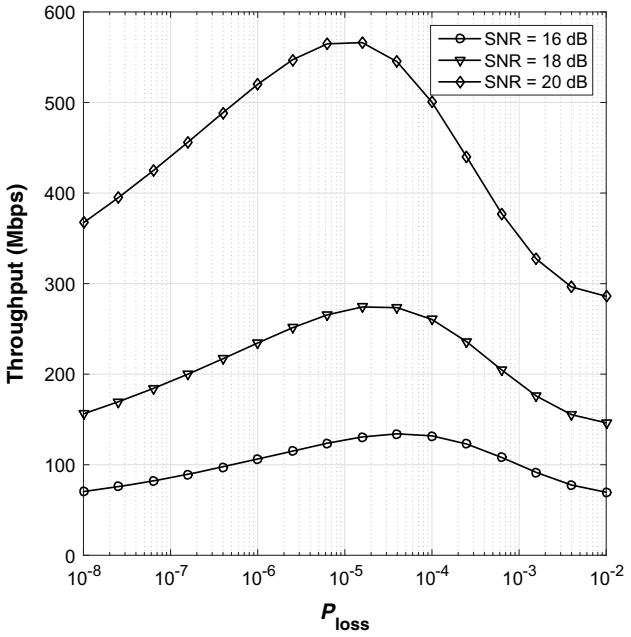

Fig. 7 TCP throughput versus average SNR with different values of P_{loss}, given $C_n^2 = 3 \times 10^{-14}\,\mathrm{m}^{-2/3}$, $M = 1$, $L = 1500\,\mathrm{m}$

transmission delay caused by the re-transmissions. Therefore, the required SNR remains unchanged when M reaches a threshold. In our case, we recommend that $M = 2$ is the optimized value under the effects of moderate turbulence channel.

The TCP performance is also studied in Fig. 7 under different conditions of the QoS. In particular, we plot the TCP throughput with respect to different values of P_{loss}

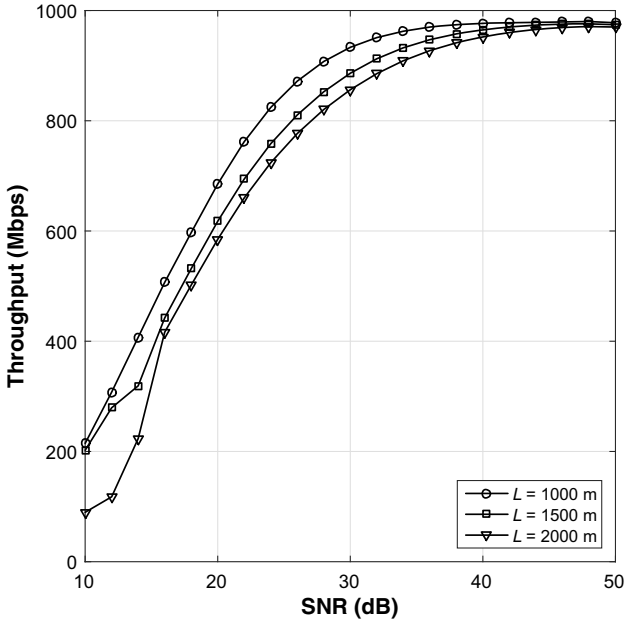

Fig. 8 TCP throughput versus average SNR with different values of channel distance, given $C_n^2 = 8.10^{-15}\,\mathrm{m}^{-2/3}$, M=1, $P_{\mathrm{loss}} = 10^{-4}$

(or the target frame error rate according to (5)), for given $C_n^2 = 3 \times 10^{-14}\,\mathrm{m}^{-2/3}$, $M = 1$, and $L = 1500\,\mathrm{m}$. It is very interesting to see that for a given value of SNR, as P_{loss} increases the throughput increases, and after reaching a maximum value, it decreases. This is because the considered SNR is quite high, and therefore, the system can have more chances to select modes with higher transmission rates for higher values of P_{loss}, while still maintaining a predefined requirement of system errors. Nevertheless, when P_{loss} reaches a threshold ($P_{\mathrm{loss}} = 10^{-5}$ for SNR = 20 dB, for example), the system error rate meets the requirement, and hence, the throughput starts decreasing if P_{loss} keeps increasing. In this example, the observed maximum throughput is 566 Mbps.

We finally discover how the channel distance impacts the TCP throughput performance via Fig. 8. It is understandable to observe that the considered system with a longer distance needs more power (or higher SNR) to achieve the same throughput in comparison with that with a shorter one. This is because for a given level of the SNR, the longer the distance, the higher the frame error rate.

6 Conclusions

A comprehensive cross-layer analysis for the TCP performance over FSO links with the impacts of ARQ and AMC schemes was studied in this paper. Different from previous works, the TCP throughput was accurately analyzed and evaluated in a Markov error model to cope with the correlation between consecutive block transmissions. The obtained

results revealed the relation between the TCP throughput and three groups of parameters, i.e., (i) its own parameter (window size), (ii) channel-dependent parameters (distance, turbulence strength, SNR) and (iii) parameters of adaptation technologies (maximum number of re-transmissions and target FER).

We further saw that the last group of parameters was designable, which could be easily controlled to improve the TCP performance. For example, we could determine the optimal target FER so that the TCP throughput was maximized. Moreover, since the last two groups were in physical and data link layers, it required a minimal cross-layer information (only the first group needs to be transferred from the transport layer to the lower layers) to determine the optimal target FER. Therefore, by simply adding the corresponding functions for cross-layer information exchange, this cross-layer design could be implemented in existing systems for a considerable improvement of the TCP throughput.

References

[1] O'Brien, D., Katz, M.: Optical wireless communications within fourth-generation wireless systems. IEEE/OSA J. Opt. Netw. **4**(6), 312–322 (2005)

[2] Zhu, Z., Kahn, J.M.: Free-space optical communication through atmospheric turbulence channels. IEEE Trans. Commun. **50**(8), 1293–1300 (2002)

[3] Mai, V.V., Thang, T.C., Pham, A.T.: Cross-layer design and analysis for FSO links using automatic repeat request and adaptive modulation/coding schemes. In: Proceedings of the 2014 International Symposium on Communication Systems, Networks, and Digital Signal Processing (CSNDSP 2014), pp. 1176–1180. Manchester, United Kingdom (2014)

[4] Khalighi, M.A., Uysal, M.: Survey on free space optical communication: a communication theory perspective. IEEE Commun. Surv. Tutor. **16**(4), 2231–2258 (2014)

[5] Mai, V.V., Pham, A.T.: Cross-layer design and analysis of adaptive-rate transmission and ARQ for free-space optical communications. IEEE Photonics J. **8**(1), 1–15 (2016)

[6] Le, L., Hossain, E., Le-Ngoc, T.: Interaction between radio link level truncated ARQ, and TCP in multi-rate wireless networks: a cross-layer performance analysis. IET Commun. **1**(5), 821–830 (2007)

[7] Go, K.C., Kim, J.H., Choo, S.M.: TCP performance-aware HARQ with AMC scheme. In: Proceedings of the 2011 IEEE Vehicular Technology Conference (VTC 2011), San Francisco, United States (2011)

[8] Raffaelli, C., Zaffoni, P.: TCP performance in optical packet-switched networks. Photonic Netw. Commun. **11**(3), 243–252 (2006)

[9] Lee, E.J., Chan, V.W.S.: Performance of the transport layer protocol for diversity communication over the clear turbulent atmospheric optical channel. In: Proceedings of the 2005 IEEE International Conference on Communications (IPCC 2005), Ireland, pp. 333–339 (2005)

[10] Kose, C., Halford, T.R.: Incremental redundancy hybrid ARQ protocol design for FSO links. In: Proceedings of the 2009 IEEE Military Communications Conference (IMCC 2009), Boston, United States, pp. 1–7 (2009)

[11] Mai, V.V., Thang, T.C., Pham, A.T.: Performance of TCP over free-space optical atmospheric turbulence channels. IEEE/OSA J. Opt. Commun. Netw. **5**(11), 1168–1177 (2013)

[12] NEC Corporation. Research and development of free-space optical communication. 2012 ICT Innovation Forum, http://www.soumu.go.jp/maincontent/000179889.pdf (2012)

[13] Kazemi, H., Uysal, M., Touati, F.: Outage analysis of hybrid FSO/RF system based on finite-state Markov chain modeling. In: Proceedings of the 2014 International Workshop in Optical Wireless Communications (IWOW), Madeira Island, Portugal, pp. 11–15 (2014)

[14] Zhang, Q., Kassam, S.A.: Finite-state Markov model for Rayleigh fading channels. IEEE Trans. Commun. **47**(11), 1688–1692 (1999)

[15] Chaskar, H.M., Lakshman, T.V., Madhow, U.: TCP over wireless with link level error control: analysis and design methodology. IEEE/ACM Trans. Netw. **7**(5), 605–615 (1999)

[16] Zorzi, R., Chockalingam, A., Rao, R.R.: Throughput analysis of TCP on channels with memory. IEEE J. Sel. Areas Commun. **18**(7), 1289–1300 (2000)

[17] Nguyen, C.T., Mai, V.V., Pham, A.T.: TCP over free-space optical links with ARQ and AMC: a cross-layer performance analysis. In: Proceedings of 2016 the International Conference on Advanced Technologies for Communications (ATC 2016), Hanoi, Vietnam, pp. 1039–2162 (2016)

[18] Jasem, H.N., Zukarnain, Z.A., Othman, M., Subramaniam, S.: The TCP-based new AIMD congestion control algorithm. J. Comput. Sci. Netw. Secur. **8**(10), 331–338 (2008)

[19] Mai, V.V., Pham, A.T.: Performance analysis of cooperative-ARQ schemes in free-space optical communications. IEEE Trans. Commun. **97**(8), 1614–1622 (2014)

[20] Uysal, M., Li, J., Yu, M.: Error rate performance analysis of coded free-space optical links over gamma–gamma atmospheric turbulence channels. IEEE Trans. Commun. **5**(6), 1229–1233 (2006)

[21] Gradshteyn, I.S., Ryzhik, I.M.: Table of Integrals, Series, and Products, 6th edn. Academic Press, New York (2000)

[22] Padhye, J., Firoiu, V., Towsley, D.F., Kurose, J.F.: Modeling TCP Reno performance: a simple model and its emperical validation. IEEE/ACM Trans. Netw. **8**(2), 133–145 (2000)

[23] Bonde, D., Bonde, J.: HIPERLAN/2 and 802.11a: a comparative study. In: Proceedings of the 2006 IEEE World Scientific and Engineering Academy and Society (WSEAS 2006), Canary Islands, Spain, pp. 7–11 (2006)

[24] Indumathi, G., Murugesan, K.: A cross-layer design to improve spectral efficiency in wireless networks. Int. J. Future Gener. Commun. Netw. **4**(1), 1–12 (2011)

[25] Dai, C.Q., Rao, Y., Jiang, L., Chen, Q.B., Huang, Q.: Cross-layer design of combining HARQ with adaptive modulation and coding for Nakagami-m fading channels. J. Commun. **7**(6), 458–463 (2012)

[26] Sadeghi, P., Kennedy, R.A., Rapajic, P.B., Shams, R.: Finite-state Markov modeling of fading channels. IEEE Sig. Process. Mag. **25**(5), 57–80 (2008)

[27] Peppas, K., Datsikas, C.: Average symbol error probability of general-order rectangular quadrature amplitude modulation of optical wireless communication systems over atmospheric turbulence channels. IEEE/OSA J. Opt. Commun. Netw. **2**(2), 102110 (2010)

[28] Yun, J., Kavehrad, M.: Markov error structure for throughput analysis of adapapive modulation systems combined with ARQ over correlated fading channels. IEEE Trans. Veh. Technol. **54**(1), 235–245 (2005)

[29] Mai, V.V., Tran, N.A., Thang, T.C., Pham, A.T.: Performance analysis of TCP over visible light communication networks with ARQ protocol. Wil. Trans. Emerg. Telecom. Technol. **25**(6), 600–608 (2014)

Chuyen T. Nguyen received his B.E. degree in Electronics and Telecommunications from Hanoi University of Science and Technology (HUST), Vietnam, in 2006, M.E. degree in Communications Engineering from National Tsing Hua University, Taiwan in 2008, and Ph.D. degree in Informatics from Kyoto University, Japan, in 2013. From September to November 2014, he was a visiting researcher in The University of Aizu, Japan. He received the Fellow award from the Hitachi Global Foundation in August 2016. He is currently an Assistant Professor at School of Electronics and Telecommunications, HUST. His current research interests are in areas of communications theory with a particular emphasis on RFID, MAC/PHY cross-layer design for optical/wireless communication systems.

Hoang D. Le received the B.E. degree from Hanoi University of Science and Technology, Vietnam, in 2016. He is currently working toward a M.E. degree in computer network at the University of Aizu, Japan. His current research focuses on cross-layer design and performance analysis of wireless/FSO systems.

Vuong V. Mai received the B.E. degree (Hons.) in Electronic Telecommunication Engineering from Posts and Telecommunications Institute of Technology (PTIT), Vietnam, in 2012. He received the M.S. (UoA President's Award of Excellence) and Ph.D. degrees as a Japanese Government (Monbukagakusho) Scholar in Computer Science and Engineering from The University of Aizu (UoA), Japan, in 2014 and 2017, respectively. In April 2017, he joined Korea Advanced Institute of Science and Technology (KAIST), Korea, where he is currently a Postdoctoral Fellow with School of Electrical Engineering. His general research areas include communications theory and photonics with emphasis on wireless applications. Recent research activities cover optical wireless communications and networking. He is a member of IEEE, IEICE and OSA.